

## Electronic Supplementary Material

### Multi-omics reveals protein kinase A regulation of lignocellulolytic response in *Trichoderma reesei*

Hermano Zenaide Neto<sup>1</sup>, Wellington Ramos Pedersoli<sup>1</sup>, David Batista Maués<sup>1</sup>, Lucas Matheus Soares Pereira<sup>1</sup>, Iasmin Cartaxo Taveira<sup>1</sup>, Andrei S Steindorff<sup>2</sup>, Renato Graciano de Paula<sup>3,4</sup>, Roberto N Silva<sup>1,4\*</sup>

<sup>1</sup>Department of Biochemistry and Immunology, Molecular Biotechnology Laboratory, Ribeirão Preto Medical School (FMRP), University of São Paulo, Ribeirão Preto 14049-900, SP, Brazil

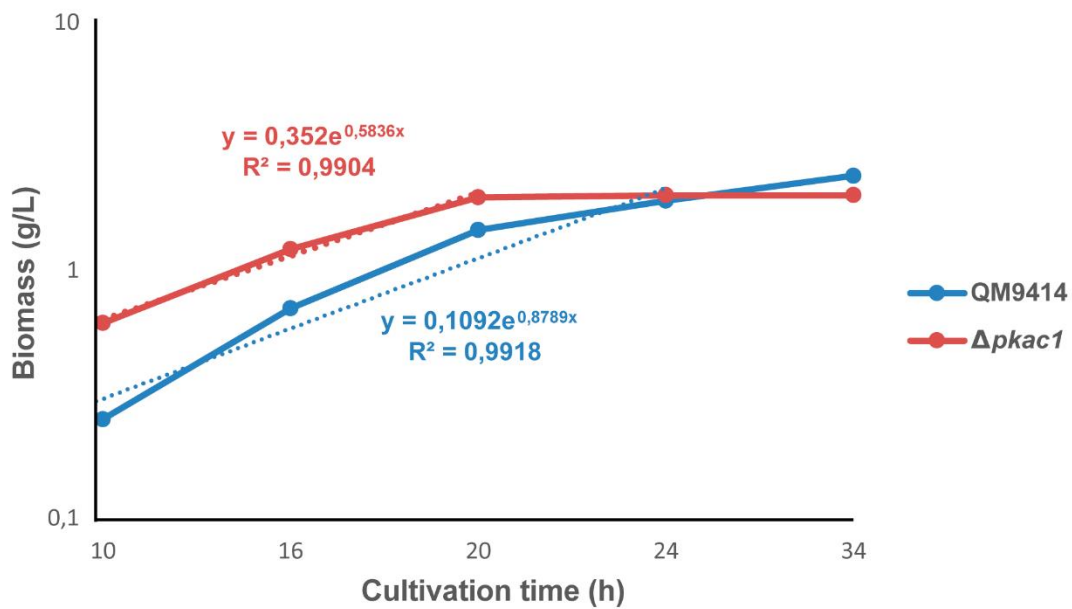
<sup>2</sup>Joint Genome Institute, Lawrence Berkeley National Laboratory, Berkeley, CA, 94720, USA.

<sup>3</sup>Department of Physiological Sciences, Health Sciences Center, Laboratory of Structural and Functional Biochemistry, Federal University of Espírito Santo, Vitória 29047-105, ES, Brazil

<sup>4</sup>National Institute of Science and Technology in Human Pathogenic Fungi, Brazil

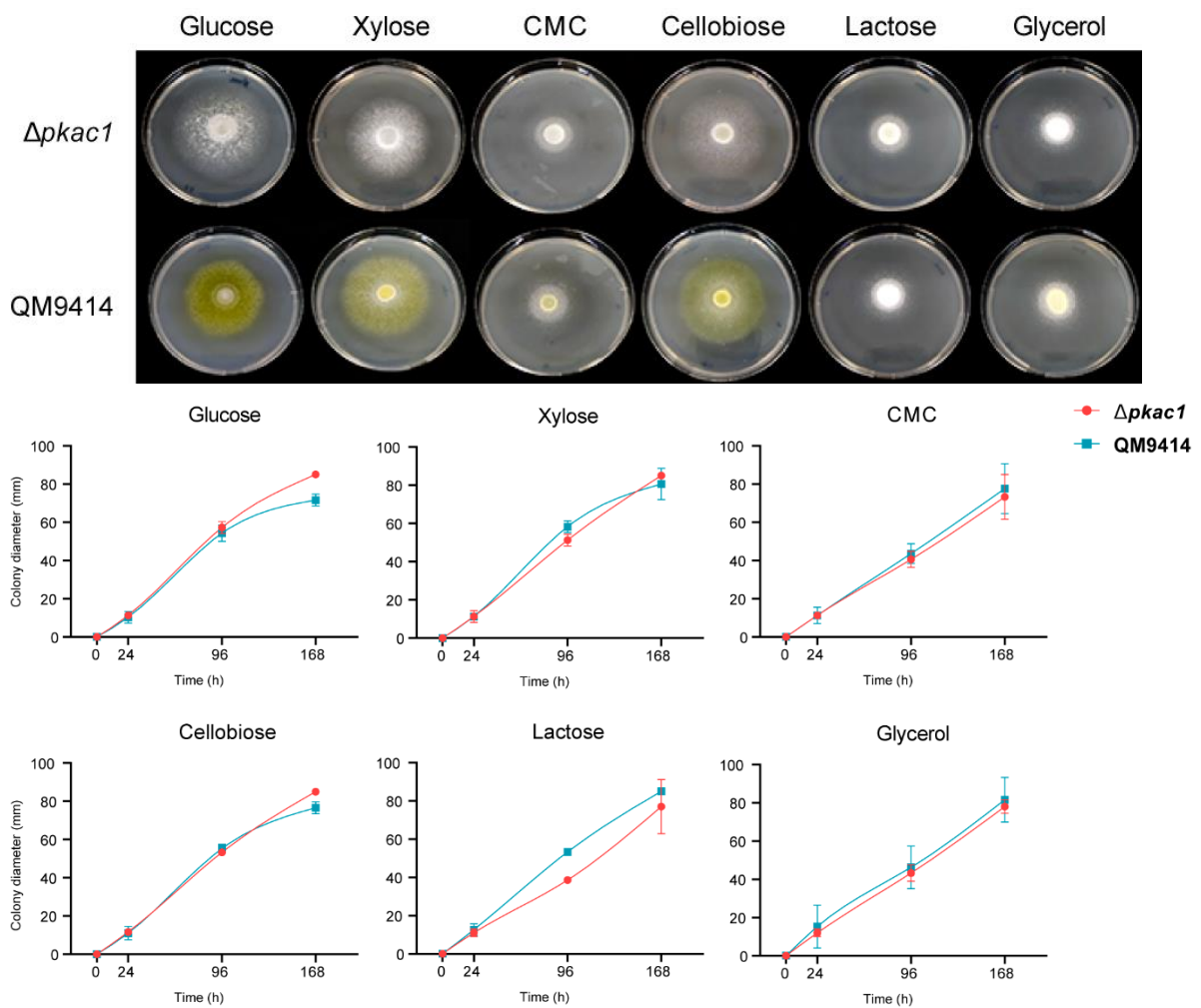
**\*Corresponding author:** [rsilva@fmrp.usp.br](mailto:rsilva@fmrp.usp.br)

**Online Resource 1.** Growth kinetics of *T. reesei* QM9414 and  $\Delta$ pkac1 in glycerol liquid medium. Strains QM9414 (blue circles) and  $\Delta$ pkac1 (red circles) were cultivated in Mandels-Andreotti medium supplemented with 1% (v/v) glycerol as the carbon source. Data points represent the mean dry biomass (g/L) of three biological replicates, with error bars indicating standard deviation. Dotted lines denote the linear regression of the logarithmic growth phase, yielding specific growth rates of  $0.1799 \text{ h}^{-1}$  for QM9414 and  $0.1506 \text{ h}^{-1}$  for  $\Delta$ pkac1.



**Online Resource 2.** Phenotypic characterization of QM9414 and  $\Delta pkac1$  strains.

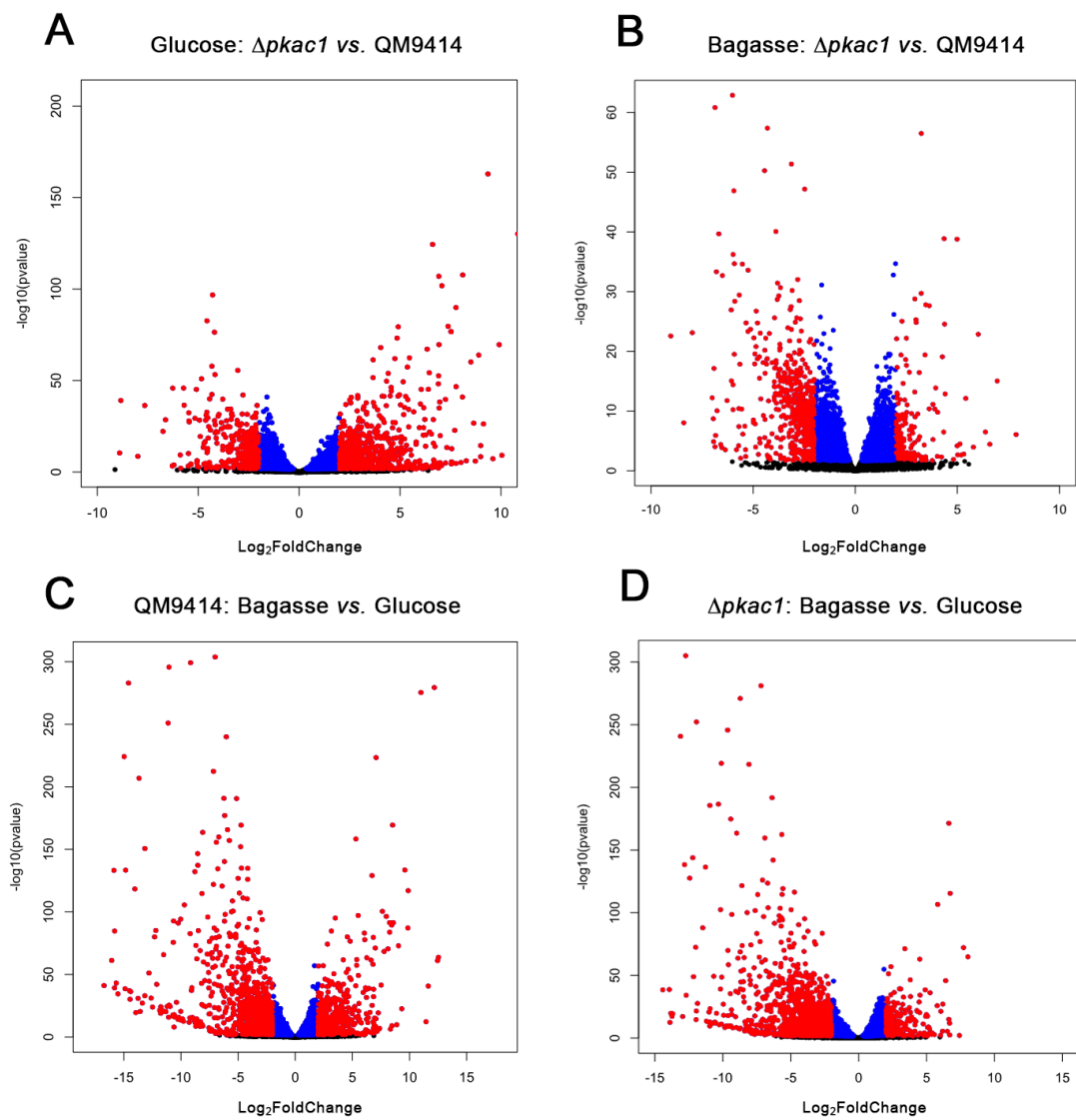
(A) Colony morphology on minimal media containing glucose, xylose, CMC, cellobiose, lactose, or glycerol (incubated for 4 days at 30 °C). Top row:  $\Delta pkac1$ ; Bottom row: QM9414. (B) Radial growth kinetics (0, 24, 96, 168 h) on the respective carbon sources; red circles =  $\Delta pkac1$ , blue squares = QM9414. Data points represent the mean  $\pm$  SD (n = 3).



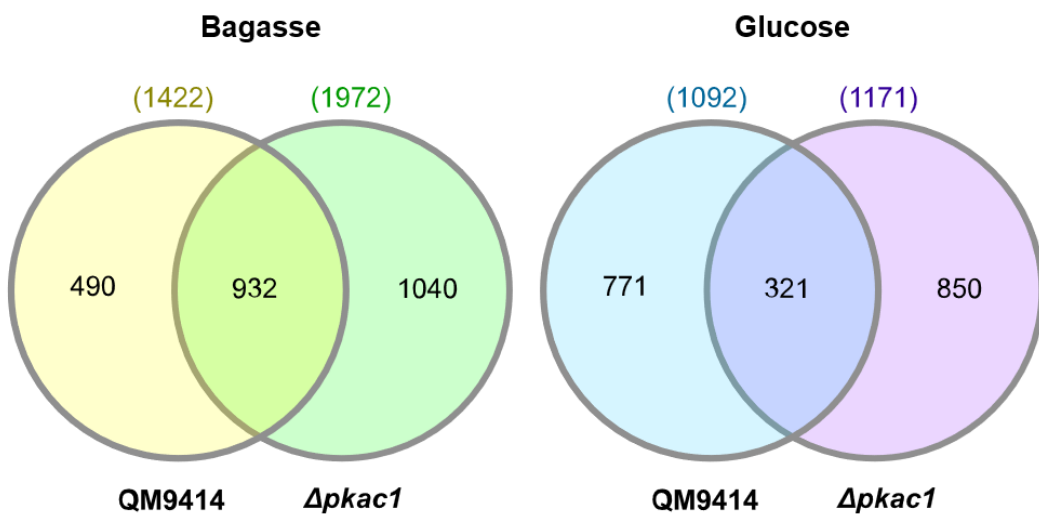
**Online Resource 3.** Principal Component Analysis (PCA) of the *T. reesei* transcriptome. The plot displays the first (PC1, 76% variance) and second (PC2, 12% variance) principal components. Each point represents an individual RNA-Seq library. Samples are color-coded by experimental group: QM9414 in glucose (red),  $\Delta$ pkac1 in glucose (green), QM9414 in sugarcane bagasse (blue), and  $\Delta$ pkac1 in sugarcane bagasse (purple). Ellipses indicate the 95% confidence interval for each group. The plot was generated in R using the *ggplot2* and *prcomp* packages.



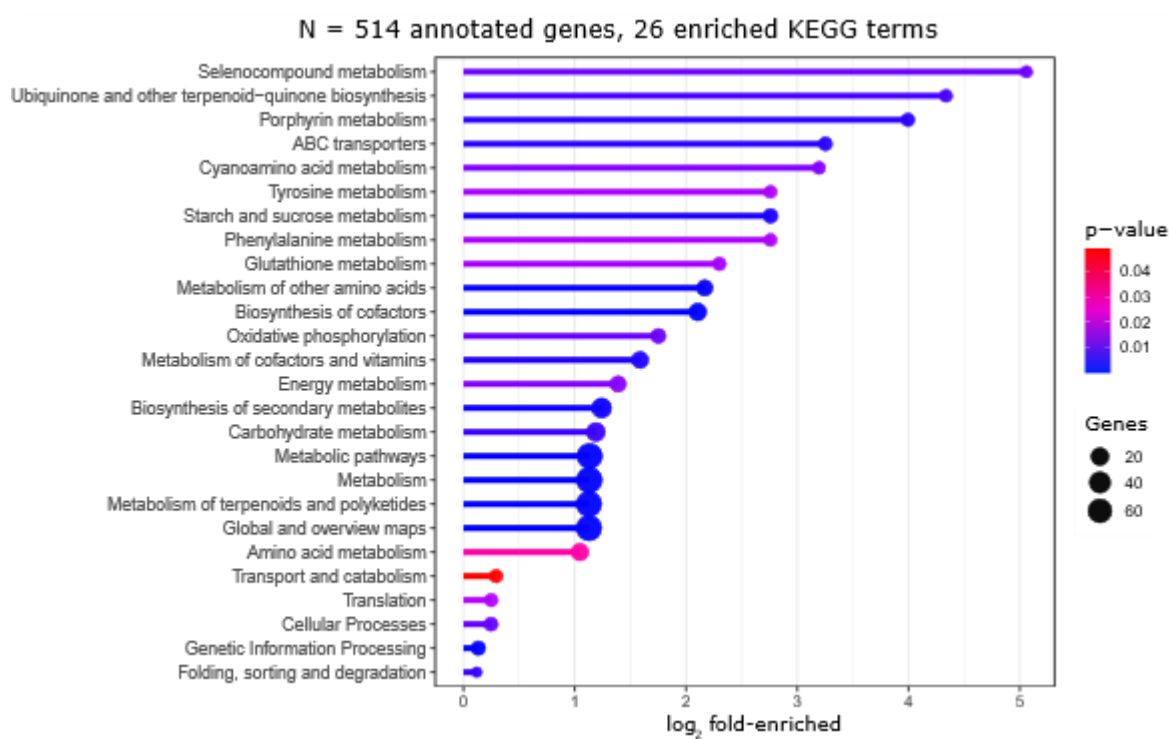
**Online Resource 4.** Volcano plots of differential gene expression. Each point represents a gene plotted according to its  $\log_2$  fold change ( $\log_2\text{FC}$ , X-axis) and statistical significance ( $-\log_{10}$  adjusted p-value, Y-axis). Differentially expressed genes (adjusted p-value  $\leq 0.05$  and  $|\log_2\text{FC}| \geq 1$ ) are highlighted in red. The four comparisons displayed are: (A)  $\Delta\text{pkac1}$  vs. QM9414 in glucose; (B)  $\Delta\text{pkac1}$  vs. QM9414 in sugarcane bagasse; (C) Bagasse vs. Glucose in QM9414; (D) Bagasse vs. Glucose in  $\Delta\text{pkac1}$ .



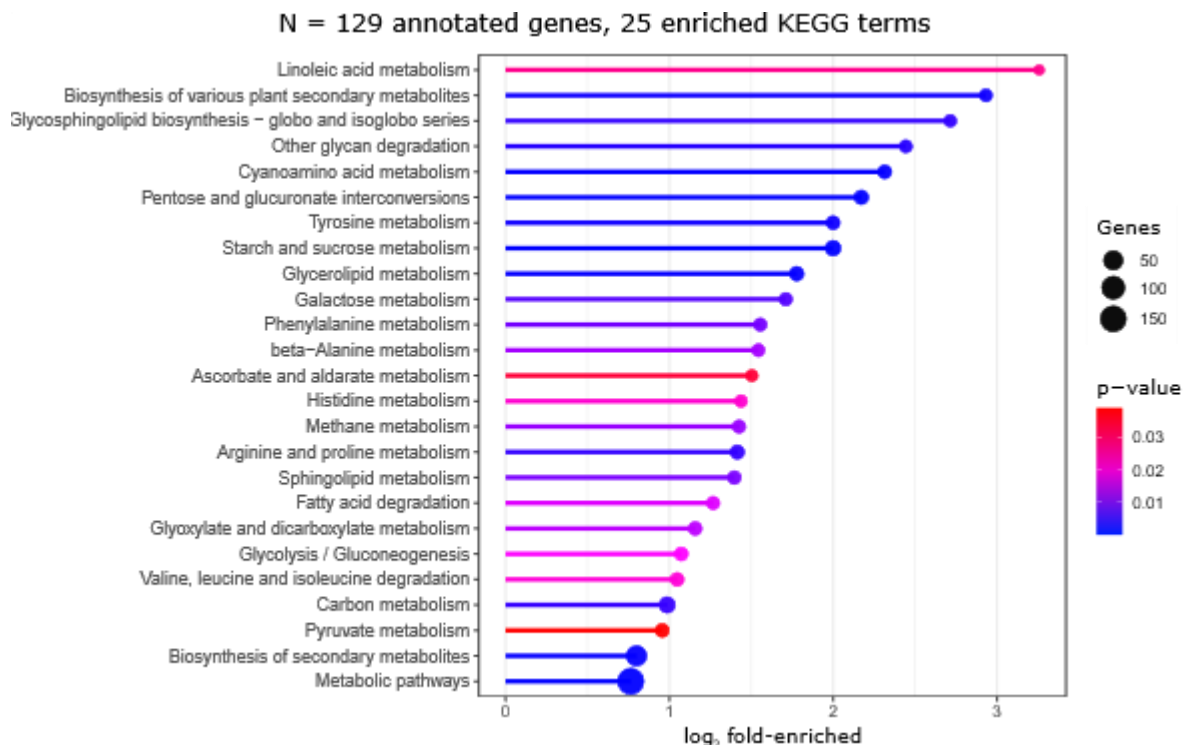
**Online Resource 5.** Venn diagrams illustrating the overlap of differentially expressed genes (DEGs) in QM9414 and  $\Delta p k a c 1$  strains under sugarcane bagasse and glucose conditions. Values in parentheses denote the total number of DEGs for that specific strain-condition. Numbers within the circles (non-overlapping areas) correspond to strain-exclusive DEGs. Numbers in the overlapping regions indicate DEGs common to both strains under the same condition.



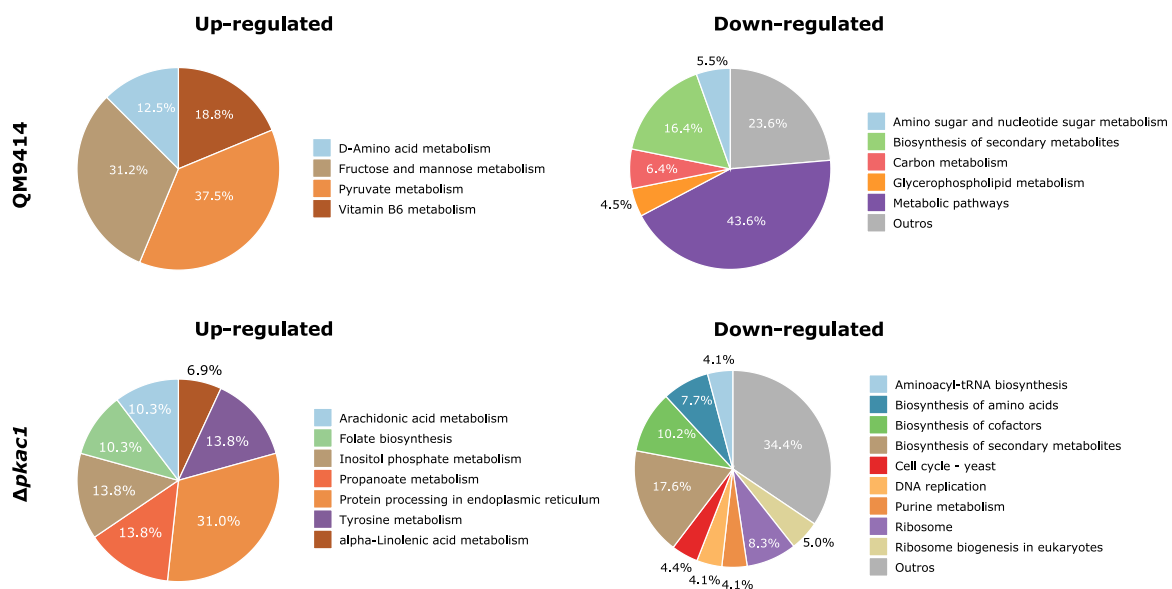
**Online Resource 6.** KEGG pathway functional enrichment of DEGs shared between the parental (QM9414) and mutant ( $\Delta pkac1$ ) strains of *T. reesei* cultivated in sugarcane bagasse. The lollipop chart displays major metabolic pathways associated with shared DEGs, including amino acid metabolism, energy metabolism, transport, biosynthesis of secondary metabolites, glutathione metabolism, and oxidative phosphorylation. Point color represents statistical significance (p-value), while point size indicates the number of genes annotated to the pathway. Line length corresponds to the degree of enrichment (Fold Enriched), and the Y-axis lists the most representative KEGG pathways. Only pathways with a p-value  $\leq 0.05$  are included.



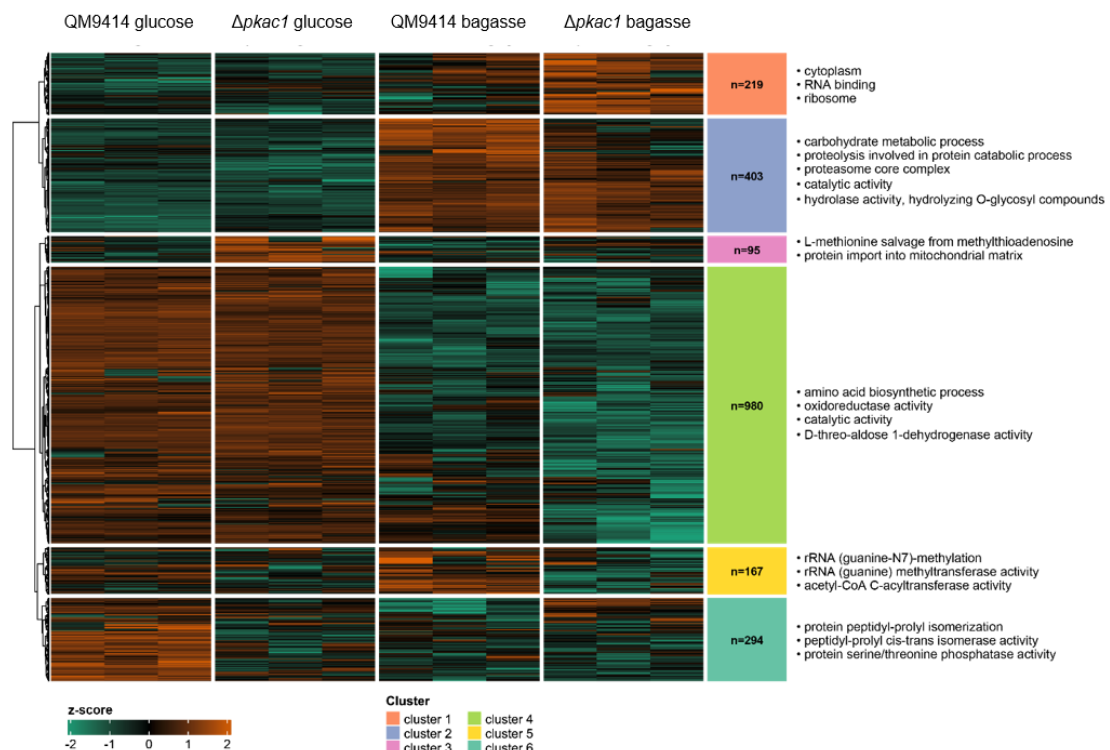
**Online Resource 7.** KEGG pathway enrichment analysis for shared differentially expressed genes in glucose. The chart shows significantly enriched metabolic pathways ( $p \leq 0.05$ ) for DEGs common to both QM9414 and  $\Delta pkac1$  strains in glucose medium. The representation follows the same scheme as Online Resource 6.



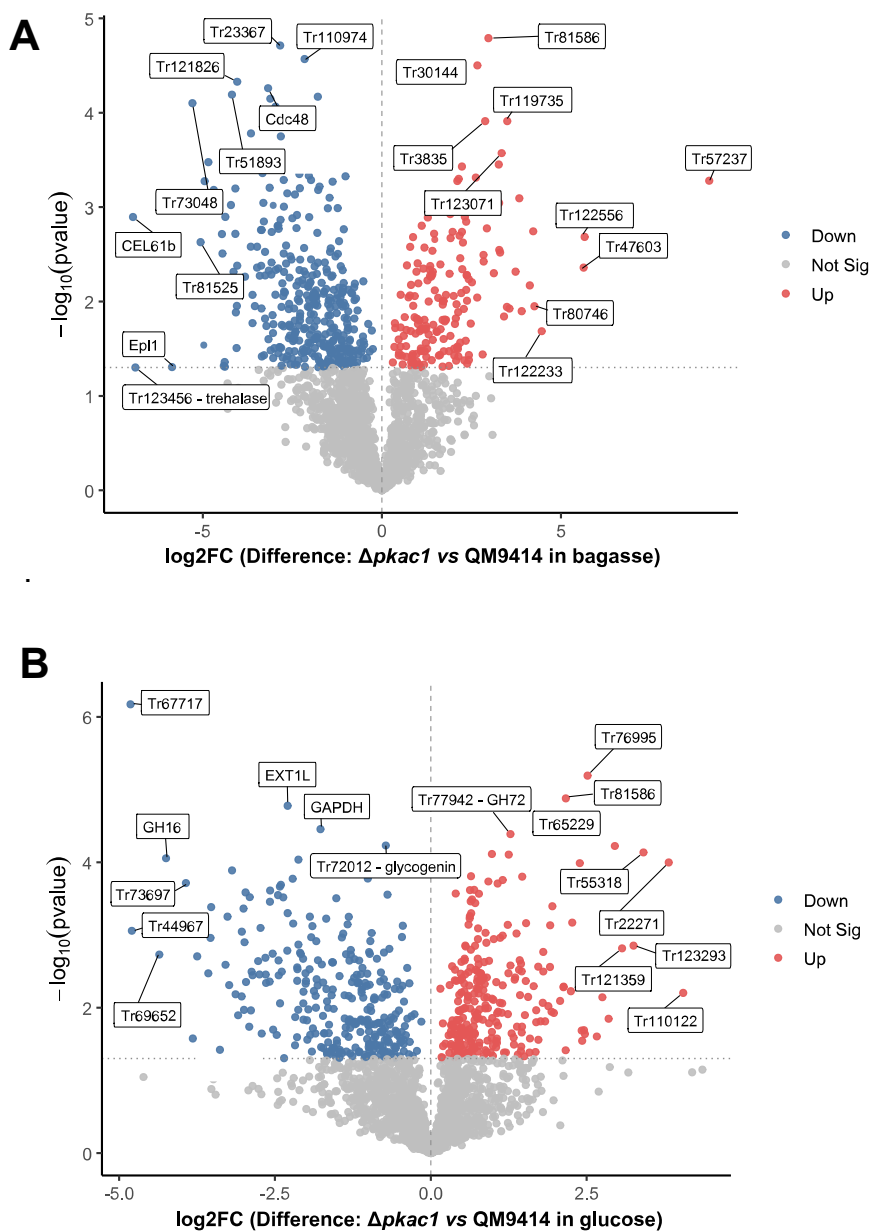
**Online Resource 8.** Functional distribution (KEGG) of strain-exclusive differentially expressed genes in response to sugarcane bagasse. Pie charts compare the distribution of functional categories for genes significantly regulated exclusively in the parental (QM9414) or mutant ( $\Delta pkac1$ ) strain when cultured in sugarcane bagasse relative to glucose. The categories represent major metabolic pathways and cellular processes, highlighting distinct transcriptional reprogramming between the two strains.



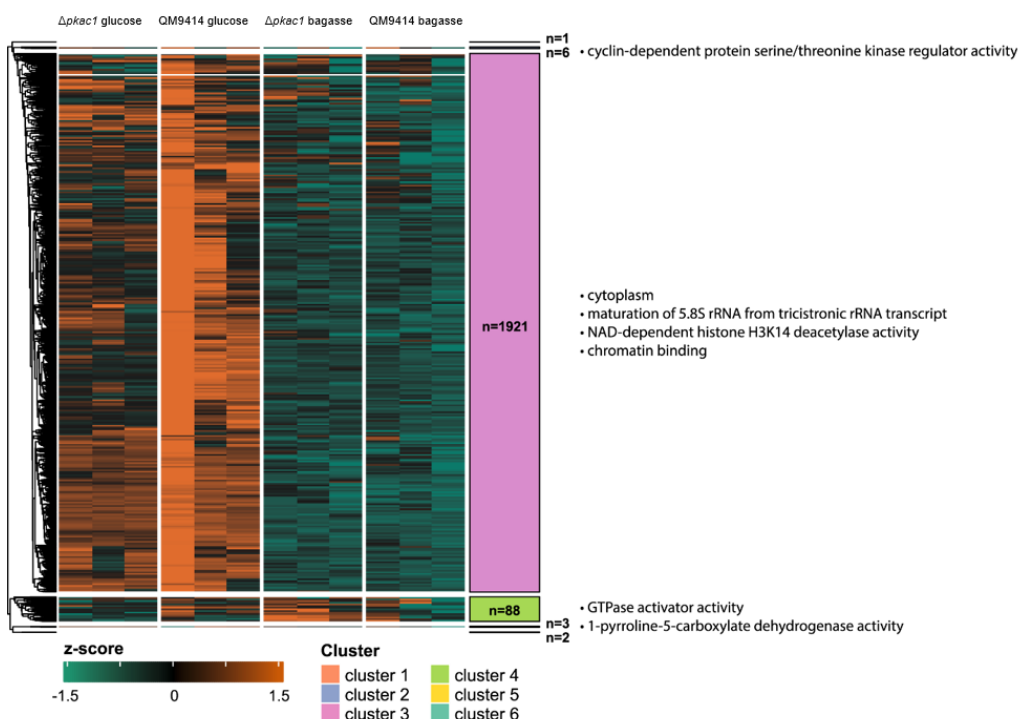
**Online Resource 9.** Hierarchical clustering heatmap of total protein relative abundance (total proteome) across culture conditions. Columns represent biological replicates for each condition. Colors indicate relative protein abundance (z-score), with green indicating lower abundance and red/brown indicating higher abundance. The lateral dendrogram clusters proteins with similar abundance profiles.



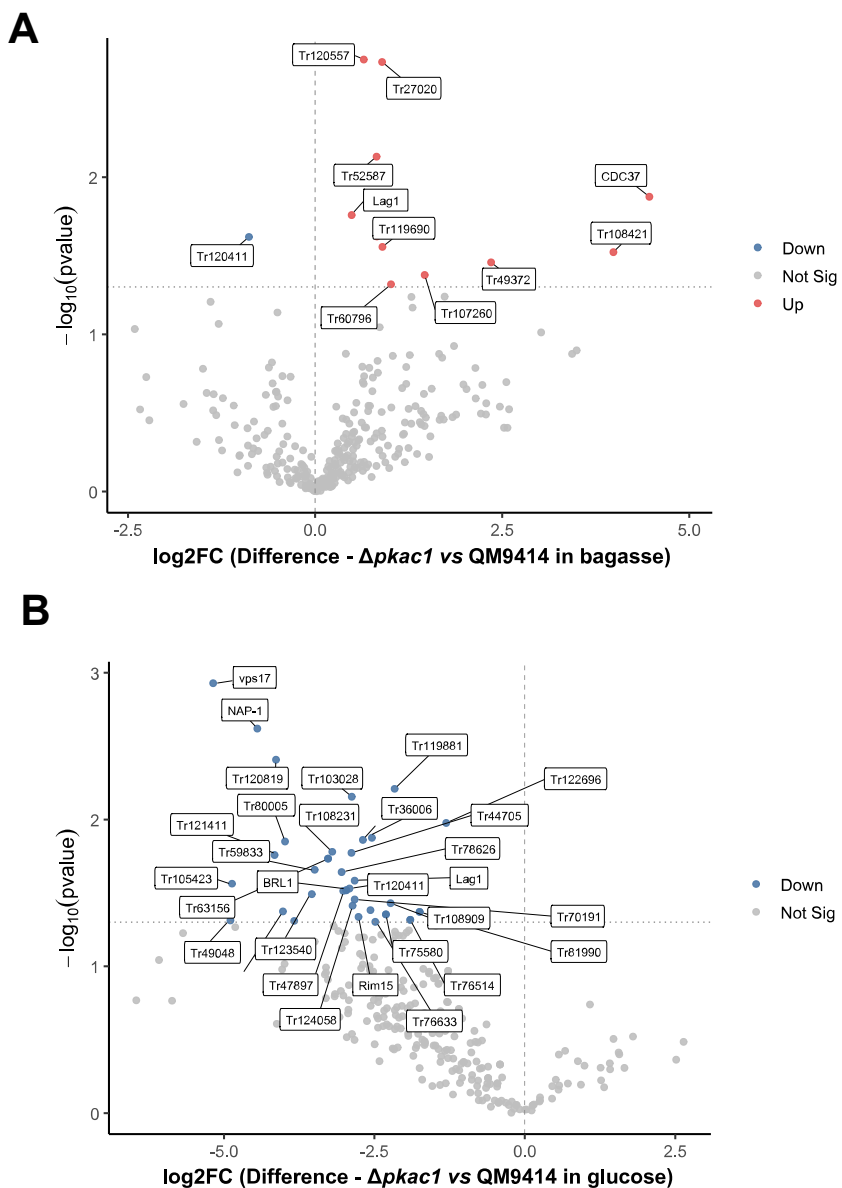
**Online Resource 10.** Volcano plots of differentially abundant proteins in the total proteome. Each point represents a protein plotted by abundance change ( $\log_2\text{FC}$ ;  $\Delta\text{pkac1}$  vs. QM9414, X-axis) and statistical significance (Y-axis). Proteins meeting the thresholds of  $|\log_2\text{FC}| \geq 1$  and  $\text{FDR} < 0.05$  are shown as significantly different, and the most strongly changing proteins are labeled. (A) Sugarcane bagasse:  $\Delta\text{pkac1}$  vs. QM9414. (B) Glucose:  $\Delta\text{pkac1}$  vs. QM9414.



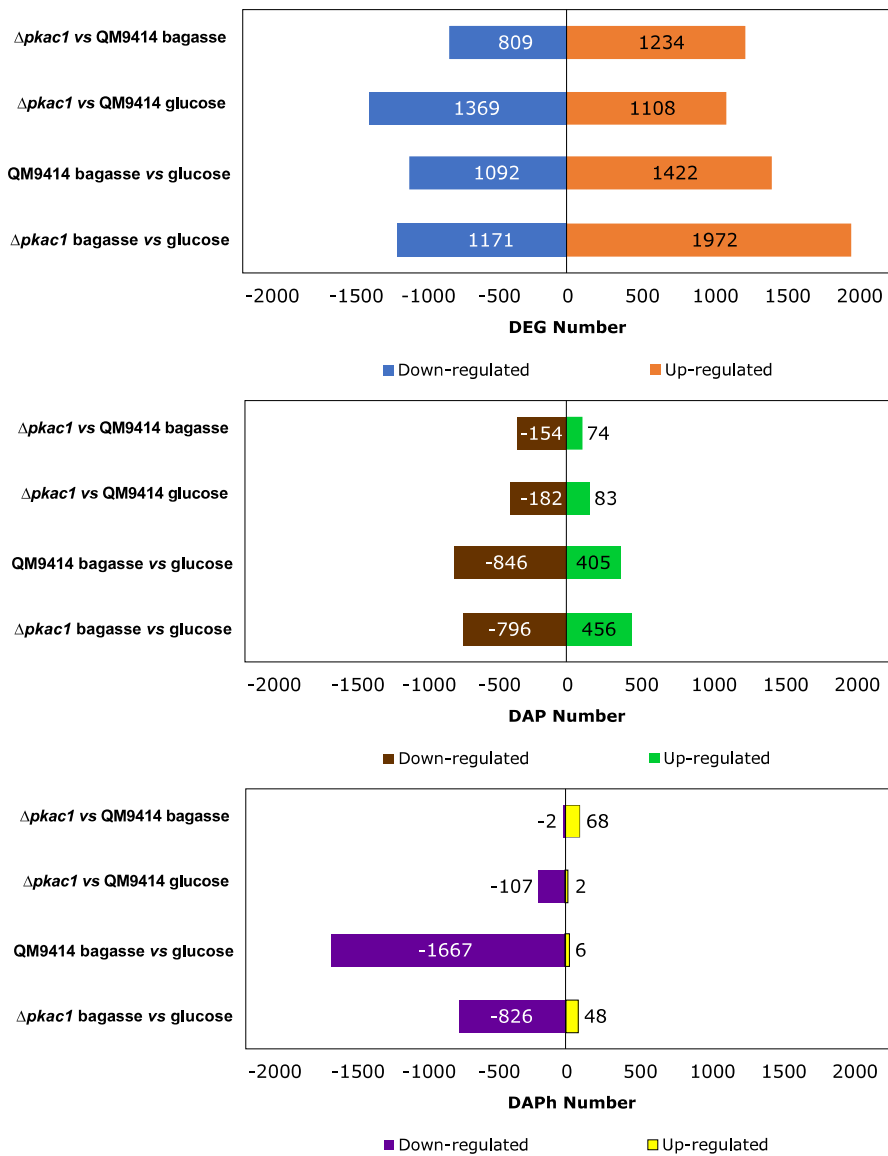
**Online Resource 11.** Phosphoproteomic landscape of *T. reesei* QM9414 and  $\Delta$ pkac1 in glucose and sugarcane bagasse. The heatmap groups phosphorylation sites based on their abundance profiles (z-score) across biological replicates for each condition. Rows represent phosphosites, and columns represent samples. Cluster analysis (right sidebar) reveals groups of sites with similar behavior and their respective most significant functional enrichments ( $p \leq 0.05$ ).



**Online Resource 12.** Differential phosphorylation analysis of potential PKA targets. Volcano plots illustrate changes in the phosphorylation status of proteins containing the PKA consensus motif (R-R/K-x-S/T). The analysis compares the mutant ( $\Delta pka c1$ ) against the parental (QM9414) strain in (A) sugarcane bagasse and (B) glucose. The X-axis represents abundance change ( $\log_2 FC$ ), and the Y-axis indicates statistical significance, with labels highlighting representative targets.



**Online Resource 13.** Quantitative overview of differential regulation across omics layers. Bar charts compare the number of up- and down-regulated elements in four experimental contrasts using cutoffs of  $\log_2\text{FC} \geq 1$  and  $\text{FDR} \leq 0.05$ . Each panel represents an analysis layer: differentially expressed transcripts (DEGs), differentially abundant proteins (DAPs), and phosphoproteins with differentially abundant phosphorylation sites (DAPhs).



**Online Resource 14.** Top candidates for direct PKA substrates identified by phosphoproteomics. The table lists proteins exhibiting the most significant reduction in phosphorylation levels in the  $\Delta pKac1$  strain that contain the PKA consensus motif.

Id	Contrast	Protein	Phosphorylated	Site Window	Score	
			Position			
Tr120411	$\Delta pKac1$ x QM9414 em Bagasse		517	S	HRRKSSTHH	0,872
Tr43877	$\Delta pKac1$ x QM9414 em Glucose		1824	S	KRRDSTTST	0,87
Tr120819	$\Delta pKac1$ x QM9414 em Glucose		206	S	VRRLSDDGA	0,854
Tr121214	$\Delta pKac1$ x QM9414 em Glucose		132	S	RRRYSEFAS	0,847
Tr76037	$\Delta pKac1$ x QM9414 em Glucose		448	S	LRRLSSSSF	0,839
Tr78626	$\Delta pKac1$ x QM9414 em Glucose		226	S	TRRESIVRR	0,713

**Online Resource 15.** Summary of peptide-*Pkac1* docking simulations. The table summarizes simulation scores for each candidate peptide. "Score (rank1)" indicates the score of the pose with the best energy, and "ΔScore" represents the difference between this score and the PKAr1 control.

Protein Id	Score (rank1)	Top-5 Median	ΔScore
Tr76037	-224,523	-189,195	16,615
Tr120819	-220,784	-215,72	20,354
Tr120411	-216,953	-205,352	24,185
Tr43877	-208,246	-203,674	32,892
Tr121214	-198,642	-175,905	42,496
Tr78626	-198,49	-194,464	42,648
PKAr1	-241,138	-204,148	0